Lawrence Berkeley National Laboratory
Lawrence Berkeley National Laboratory

Title
AN EVALUATION OF THE ERC VIRTUAL IMPACTOR

Permalink
https://escholarship.org/uc/item/6rt5w3ck

Author
Loo, Billy W.

Publication Date
1974

eScholarship.org Powered by the California Digital Library
University of California

RECEIVED
LAWRENCE
RADIATION LABORATORY

MAR 29 1974

LIBRARY AND
DOCUMENTS SECTION

LBL-2468
UC-4 Chemistry
TID-4500-R61

c.2

AN EVALUATION OF THE ERC VIRTUAL IMPACTOR

Billy W. Loo and Joseph M. Jaklevic

January 1974

Prepared under Interagency Agreement between the Environmental Protection Agency and the U. S. Atomic Energy Commission
Contract No. EPA-IAG-079 (D)

Also supported by the U. S. Atomic Energy Commission
under Contract No. W-7405-ENG-48

TWO-WEEK LOAN COPY

This is a Library Circulating Copy which may be borrowed for two weeks. For a personal retention copy, call Tech. Info. Division, Ext. 5545

LAW
UNIVERSITY OF
BERKELEY
LABORATORY

LBL-2468
c.2

LBL-2468

AN EVALUATION OF THE ERC VIRTUAL IMPACTOR

Billy W. Loo and Joseph M. Jaklevic
Lawrence Berkeley Laboratory
University of California
Berkeley, California 94720

ABSTRACT

Measurements have been made on a dichotomous virtual impactor developed by the Environmental Research Corporation. The object was to study the feasibility of employing the virtual impaction scheme in air samplers to collect size fractionated particle samples for subsequent X-ray fluorescence analysis. The size separation characteristics and losses as a function of particle size at specific locations within the apparatus have been determined. It was found that except for the intrinsic losses near the size cut point, most of the losses can be significantly reduced with improved design. The propsect of large scale deployment of virtual impactors for continuous air monitoring is favorable.

AN EVALUATION OF THE ERC VIRTUAL IMPACTOR*

Billy W. Loo and Joseph M. Jaklevic

Lawrence Berkeley Laboratory
University of California
Berkeley, California 94720

INTRODUCTION

The elemental analysis of atmospheric particulates by X-ray fluorescence requires samples to be collected in the form of a thin uniform layer on a light substrate. The fact that typical urban aerosols have a characteristic distribution of particle sizes makes it desirable to collect several samples distributed over the size spectrum. Conventional aerodynamic size fractionators in the 1 micron size range generally utilize the well studied principle of particle impaction by a jet on a deflecting plate.[1,2] The particle deposits in these impactors are necessarily in the form of an image or images of a small slit or circular holes. The situation is further hampered by particle bounce and blow-off phenomina. A virtual impactor, however, aims at circumventing these problems that are characteristic of real impactors by requiring particles to be 'impacted' through a hole in the deflecting surface and be subsequently collected uniformly on a filter.

The Environmental Research Corporation has developed a dichotomous virtual impactor with a 2 micron size cut for the EPA. The object of this evaluation is to determine the feasibility of large scale deployment of such virtual impactors in automated air

samplers for X-ray fluorescence analysis. The size separation characteristics and losses as a function of particle size are to be specifically determined.

DESCRIPTION OF APPARATUS

Figure 1 is a photograph of a dissembled ERC virtual impactor showing the various components, and Fig. 2 is a simplified assembly drawing.

The aerosol is drawn through the three entrance holes in the part labeled B (referring to denotations in Fig. 2) at a total rate of 50 ℓ/min. The diameter of the holes in parts B and F are 3.96 mm and 2.18 mm while the 'impaction distance' to jet diameter ratios are 0.45 and 0.75 respectively for the two separating stages. Thus the corresponding jet Reynolds numbers are 5900 and 1500. The combination of the hole in part F and those around the flange on part E is to distribute the internal flow such that only one seventh of the total flow is allowed through the inner tube E. Particles which cannot negotiate the turns around the lips of the protruding tubes in part D will be carried down into the inner tube. The process is repeated in a similar fashion at the lower section of the apparatus where the flow through tube K is maintained at 1 ℓ/min. Thus large particles above the size cut at 2 micron unit density Stoke's diameter along with about 2% of the small particles will be collected on filter A. Most of the small particles will be carried by the main flow at 49 ℓ/min and collected on filter B.

METHOD

Due to the close approximation of their geometric diameters to unit density Stoke's diameters, dioctyl phthalate (DOP) droplets, having a specific gravity of 0.98 are best suited to serve as test particles. They are generated in a Berglund-Liu monodisperse aerosol generator with uranine (fluorescein sodium) used as a tracer for quantitative measurements. Particle losses at various points within the impactor can be best determined by washing off the aerosol deposition from a particular region of interest. The uranine content of the solution is then measured by UV fluorescence techniques.

Figure 3 is a schematic of the U.V. fluorescence analyzer. A 76-mm diameter pyrex dish holds the sample solution. The central portion of the solution is viewed by a photomultiplier via a mirror such that edge effects and U.V. attenuation in glasswares are avoided. The signal-to-background ratio is greatly enhanced by the use of complementary filters: one at the mercury light source with a transmission band from 2500 A to 4000 A and the other (green X1) in front of the photomultiplier. This scheme also renders measurements practically immune to U.V. scattering by dust or DOP itself. The filter combination is not optimized for maximum sensitivity but rather it yields an adequate and convenient operational level. With the aid of fiber optics, the stability of the analyzer is monitored by maintaining a fixed source-detector transfer function which is checked before and after each measurement by means of a sliding shutter.

PROCEDURES

The virtual impactor must be operated in a vertical configuration since gravitational effects are not neglegible for large particles in regions of low flow rate. A Gast carbon vane pump (Model 0522-103-G18D) operating at 1725 rpm is used. The total flow rate of 50 ℓ/min is monitored with a manometer which is calibrated with a temperature compensated integrating flow meter. The rate through filter A is maintained at 1 ℓ/min by an inline flow meter.

DOP particles of 1 to 10 micron diameters are produced by a Berglund-Liu monodisperse aerosol generator. A liquid jet is produced by forcing a solution of the particulate matter in a volatile solvent through an orifice with a syringe pump. A periodic disturbance is imparted to the liquid jet by vibrating the orifice with a piezoelectric ceramic. Operating in the proper region of instability of a liquid jet, the eventual size of the particle depends on four influencing factors:

i) The feed rate of the syringe pump.

ii) The vibrational frequency of the orifice.

iii) The concentration of non-volatile solute.

iv) Any void fraction in the residual particle upon evaporation of the original droplet.

For consistant operations, a single calibrated feed rate of 1.3307×10^{-3} ml/s and a vibration frequency of 144.60 KHz are used to generate initial droplets of 26 microns with a 10 micron orifice. The solutions used consist of one part by volume of demineralized water to 14 parts of isopropryl alcohol with 50 μg/ml of uranine

and selected amounts of DOP according to the final particle size desired. Such droplets are then dispersed and dried by dehumidified compressed air and are charge neutralized by a 10 mc Krypton-85 source. The uniformity of the aerosol is checked by visual observation of the initial droplet stream as deflected by a transverse air jet. With the aid of a scanning electron microscope, samples of individual particles are examined for size and void fraction estimations.

Since the sizes of small particles are significantly affected by the amount of impurities present in the solution, the syringes are ultrasonically cleaned with detergents and followed by water and alcohol rinses. Thus impurities essentially consist of 10 μg/ml of alcohol residue and 50 μg/ml of uranine.

For each test run, the loss profile is determined from washings of depositions from six designated regions: (1) parts B and C, (2) part D, (3) the inside wall of tube E, (4) parts F and G, (5) part H, and (6) part K. A slight amount of loss in the connecting tube to filter B is included in the filter B measurement. Uranine, being very soluble in water, is retrieved readily from the depositions on 0.8 micron Millipore filters. For DOP droplets greater than 5 microns, a few seconds of ultrasonic agitation will facilitate complete retrieval.

RESULTS

A number of calibration and monitoring functions have been exercised to minimize instrumental errors. The average sampling rate as determined from total integrated flow for all the test runs is 49.75 ℓ/min with an rms deviation of 1.2%. This represents the stability of sampling rate without feedback control; although some initial adjustments are needed for different filters.

The average feed rate of the syringe pump is 1.3307×10^{-3} ml/s with an rms deviation of 0.3% for different syringes. The 144.60 KHz frequency is applied to the vibrating orifice and is continuously monitored and exhibits less than 0.1% deviations. With careful preparation of solutions used for generating aerosols, the overall error on the particle size is probably 1% in cases where the uncertainties due to impurities is not a dominating factor.

Since the absorption and emission bands of fluorescein sodium partially overlaps, the effect of self-absorption will be very significant for concentrated solutions. Figure 4 shows a plot of detector output current vs. uranine concentration obtained with seven dilutions of a common sample. A least square fit to the calibration data gives

$$I = 0.4723\ (1-\exp\ (-42678x))$$

where I is the photomultiplier anode current in microampere and x is the uranine concentration in gm/cm^2. A constant background of 5.6×10^{-10} amp is subtracted from each measurement. This yields an effective attenuation length of 58.43 $\mu g/cm^2$ defined as the

concentration at which 63% of the radiations is absorbed. The detection limit at 95% confidence level is 1 ng/cm^2, corresponding to approximately 10 ng in the sample. A typical test run collects about 10 micrograms of the tracer; at such level self-absorption has no significant effect.

Table 1 is a summary of the percent deposition of DOP on various parts of the sampler and filters for incident particle sizes between 1 to 10 microns. The particle sizes are expressed in terms of unit density Stoke's diameters. They reflect the corrections for 50 μg/ml of uranine and 10 μg/ml of solvent residue which are taken to have a bulk density of 1.7 gm/ml and an estimated void fraction of 48% from scanning electron microscope observations. The 1.06 micron particles consist of mainly uranine with no DOP. The size corrections for 1 and 1.5 micron DOP for example are 21% and 8% respectively.

DISCUSSION

Figure 5 is a graphical illustration of the experimental results. The structure in the loss spectrum is derived from the composite of its various smoothed components. The loss spectrum due to a single contributing mechanism is expected to have a smooth variation with particle size.

Figures 6 through 11 are the plots for the six loss regions. It is observed that for region 1, the peak at small particle sizes is due to the ring shaped deposition around the holes on the underside of part B, as can be seen in Fig. 1. Such depositions

are believed to be the results of direct impaction from the radial spacial oscillation of the streamlines rather than from eddy depositions. The oscillation is characteristic of the local geometry and flow rate. Similar phenomena have been observed in rectangular impactors where a succession of line deposits appear about an impaction slit.[3] Note also that one of the three supporting legs on part D in Fig. 1 is narrower than the others. The presence of these legs in the most direct line of flow has a definite bearing on the balance of flow rate in the individual channels. Consequently, there is usually no ring deposit around the hole opposite to the narrow supporting leg, but a higher loss is found on the edge of the corresponding opening in part C. The losses at larger particle sizes are from the depositions on the upper lips of the entrance holes.

Depositions in region 2 are found mostly on the lips of the protruding tubes of part D. The impaction depositions show distinct azimuthal variations, reflecting the sensitivity of flow patterns to structural asymmetries. Part C is used to reduce the eddy losses around the tubes but some deposition is found on its circular openings.

For region 3, there is evidence that the expanding jets touch upon the adjacent walls on part E. The slightly higher loss toward larger particle sizes probably reflect the higher penetrating power of the more massive particles through the boundary layers near the walls.

Losses in region 4 bear the same nature as those in region 1. The shifting of the loss peak to a smaller size indicates that the characteristic size cut of the second stage of separation is somewhat lower than that of the first stage. The data point at 6 μm is believed to be an anomaly; this is also obvious from its deviation from the expected smooth collection curve for filter A.

The loss spectrum for region 5 should behave similarly to region 2. Besides the slight shift of the loss peak to the smaller size, which is consistant with the parallel comparison of regions 1 and 4, there is an overwhelmingly high turbulance loss component at large particle sizes when the flow through filter A is restricted to 1 ℓ/min.

There are no distinct patterns of deposition in region 6; most of the losses probably occur in the slight mismatch to the filter holder.

CONCLUSION

It is obvious that the virtual impactor has successfully collected aerosols uniformly on two filters according to two size ranges.

The high losses near the cut region is probaby intrinsic to the virtual impaction scheme since any deflecting surface will ultimately present itself as an efficient impacting surface at some particle size. Furthermore, the boundary condition at the rigid surface of a real impactor cannot be fully realized with the presence of the collection hole. The Gaussian-like pressure

profile across the impinging jet cannot be balanced by a uniform static pressure in the collection volume. The streamlines will result in penetrating into the hole and be accompanied by a counter flow near the edges should the net flow into the particle collection volume be restrained. It is suspected that in a very confined region where such counter flow cannot be maintained, excessive turbulance will be developed. The development of such turbulance is probably responsible for the high losses at large particle sizes. On the other hand, a significant amount of loss is found to depend on details rather than principles of a virtual impactor and can be eliminated with suitable attention in design and fabrication.

In view of the fact that there will be a significant amount of irreducible losses, periodic cleaning may be required, and the apparatus should be designed for easy dismentlement and high mechanical integrity. On the other hand, a truly automated sampler should require no maintainance more frequent than perhaps on a weekly basis.

It is felt that losses may be kept to a tolerable limit with an improved design particularly when it is weighed by the bimodal natural aerosol size spectrum. It is also consoling to note that bounce-off, while being a villian in a real impactor, is a benefactor in a virtual impactor. The question whether blow off or re-entrainment will constitute a limitation can be answered more meaningfully after all reducible losses are kept to a minimum.

ACKNOWLEDGEMENTS

*This work was supported in part by the Environmental Protection Agency under Interagency Agreement with the U. S. Atomic Energy Commission Contract No. EPA-IAG-0089(D)/A.

The authors wish to express their thanks to Drs. Carl Peterson and Tom Dzubay for making the virtual impactor available, and to Dr. John Conway for the light source and detector used in the U. V. fluorescence analyzer.

REFERENCE

1. May, K. R., The Cascade Impactor: An Instrument For Sampling Coarse Aerosols, J. Sci. Instr., 22:187 (1945).

2. Marple, V. A., A Fundamental Study of Inertial Impactors, Doctoral Thesis, University of Minnesota, December, 1970.

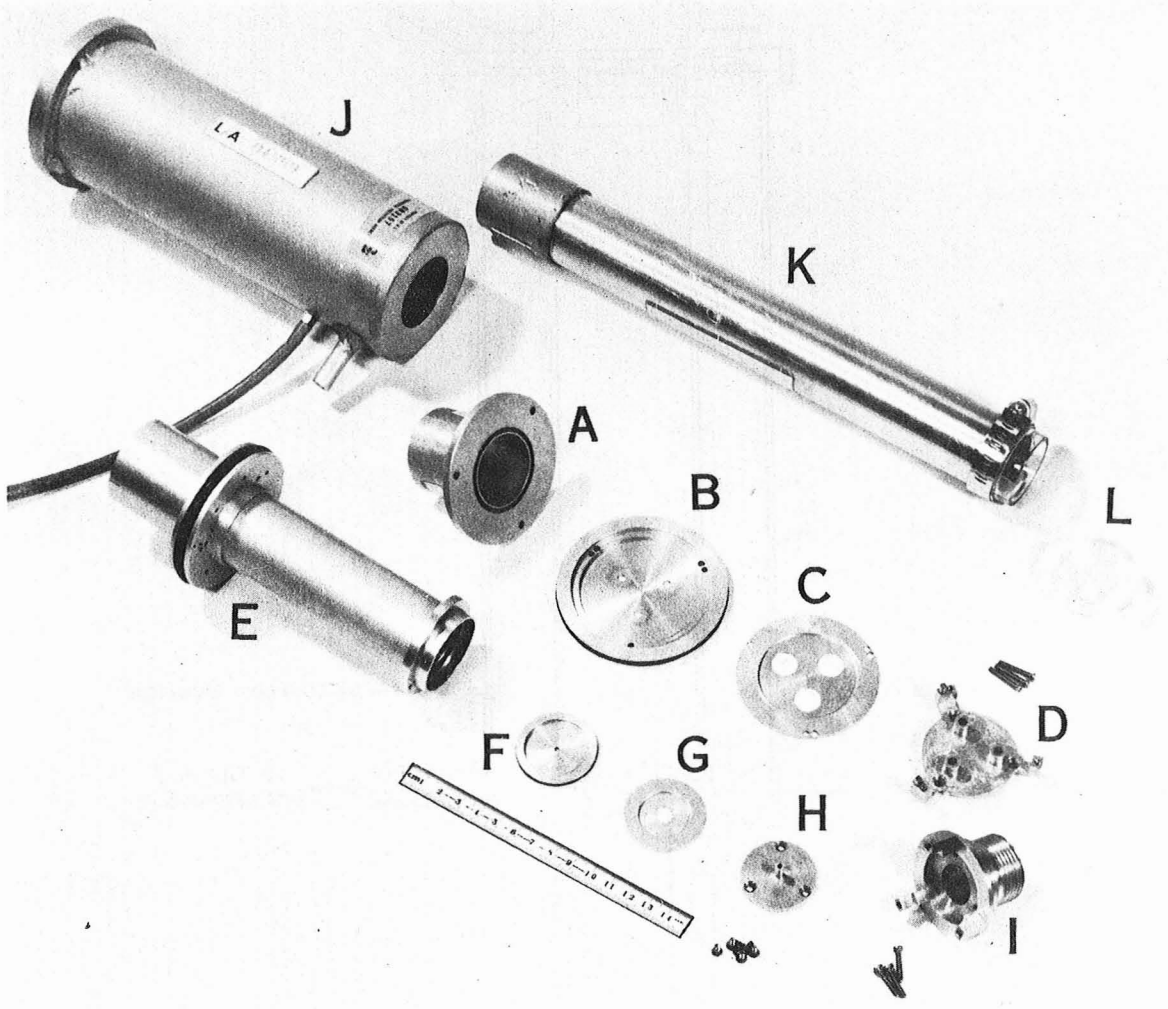
3. Axel Berner, Private Communications.

EVALUATION OF ERC VIRTUAL IMPACTOR

PERCENT DEPOSITION OF MONODISPERSE DOP ON SAMPLER AND FILTERS

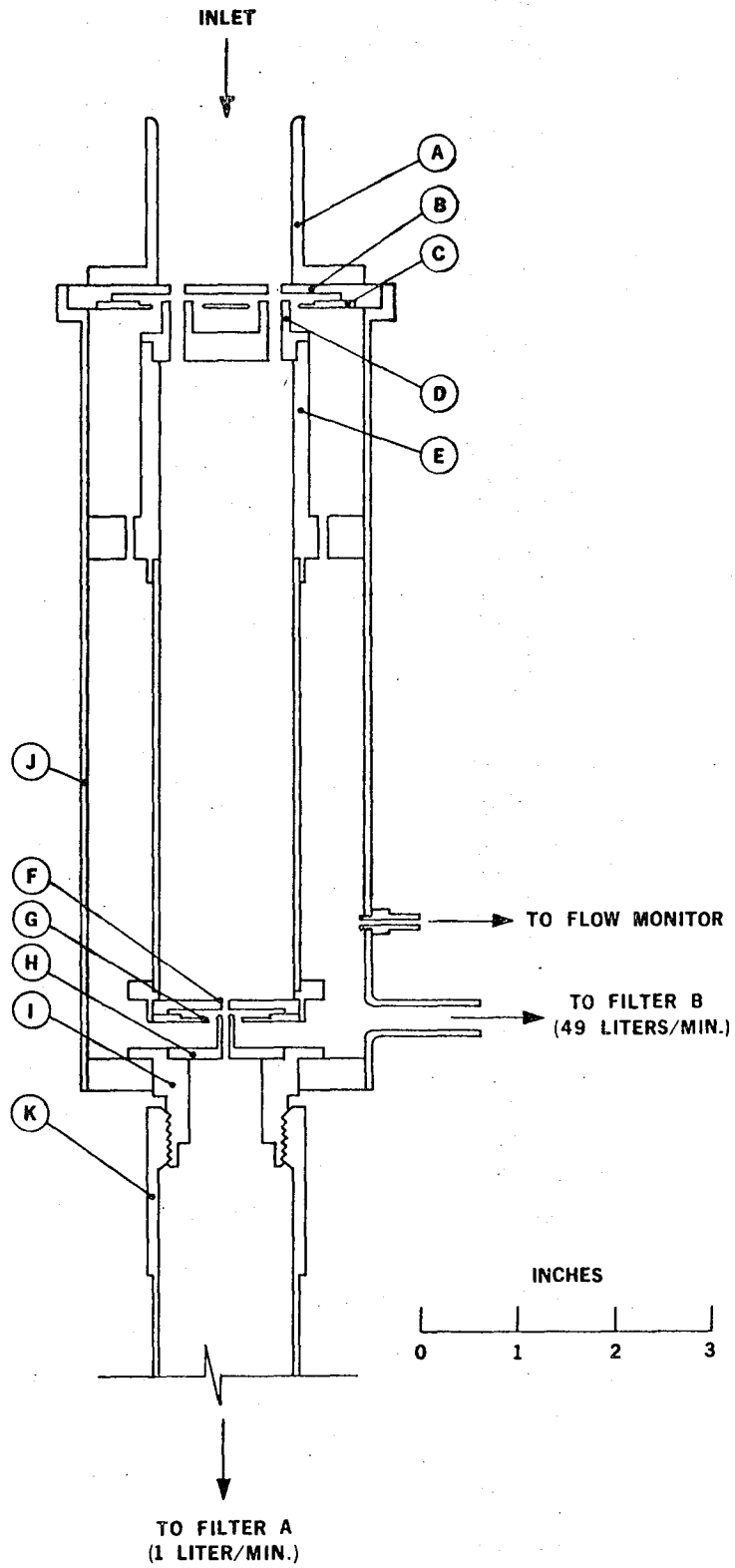
UNIT DENSITY STOKE'S DIAMETER	1.06 (μm)	1.26 (μm)	1.63 (μm)	2.08 (μm)	2.55 (μm)	3.04 (μm)	4.02 (μm)	6.01 (μm)	8.01 (μm)	8.63 (μm)	10.00 (μm)
REGION 1	4.7	4.1	10.2	11.8	9.2	0.4	0.2	0.8	2.0	2.6	4.6
REGION 2	0.1	0.2	1.3	3.2	15.3	21.9	1.2	0.1	0.6	0.4	0.8
REGION 3	0.1	0.1	0.2	0.1	0.2	0.1	0.1	0.2	0.7	0.6	1.2
REGION 4	1.8	2.9	2.0	0.9	0.9	0.7	1.1	3.2	1.6	2.4	3.5
REGION 5	0.1	0.4	11.0	8.9	0.8	0.1	0.7	0.7	2.5	8.0	32.4
REGION 6	0.1	0.2	0.2	0.2	0.5	0.4	0.5	1.2	1.9	1.6	1.7
TOTAL LOSS	6.9	7.9	24.9	25.1	26.9	23.6	3.8	6.2	9.3	15,6	44.2
FILTER A (Above Cut)	4.2	4.7	11.5	26.3	49.5	75.1	95.7	93.5	90.2	84.0	55.3
FILTER B (Below Cut)	88.9	87.2	63.5	48.7	23.5	1.3	0.4	0.3	0.5	0.4	0.4

TABLE 1



XBB 7311-6673A

Fig. 1. Components of the ERC virtual impactor



XBL 7311-6801

Fig. 2 Simplified assembly drawing of the ERC virtual impactor

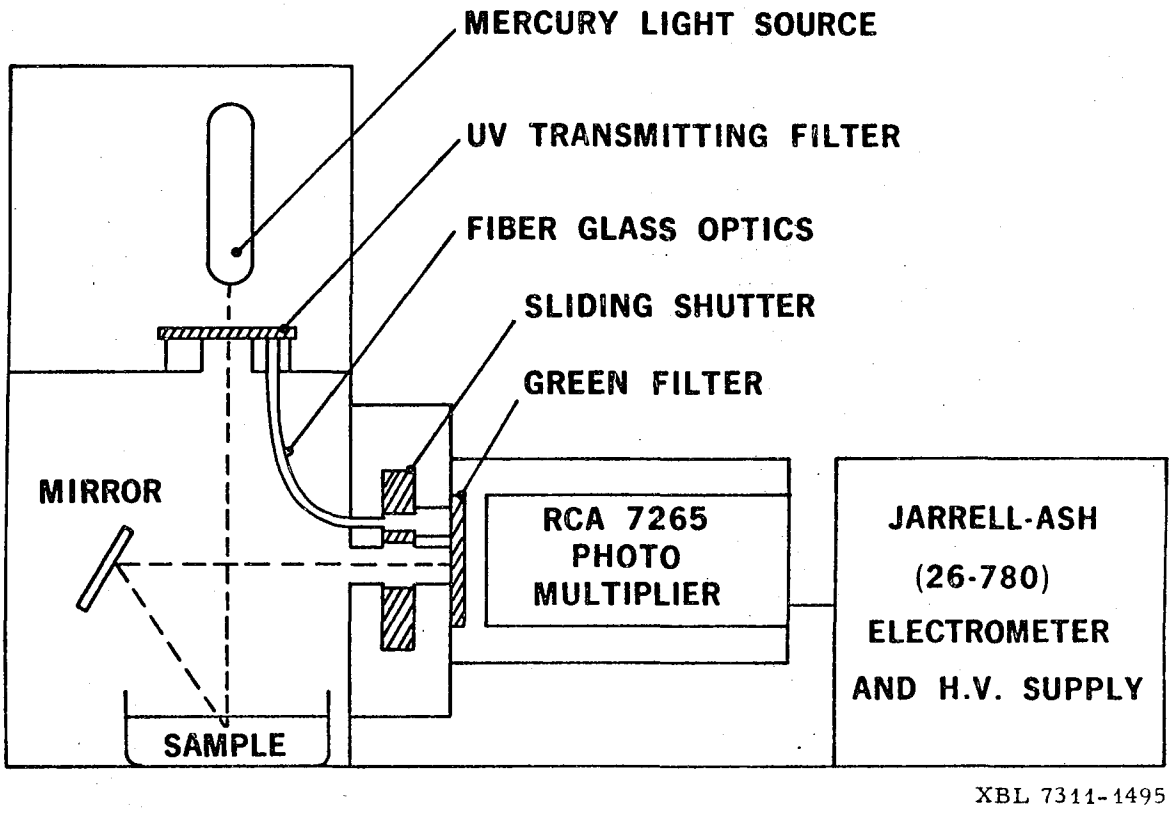


Fig. 3 U.V. fluorescence analyzer

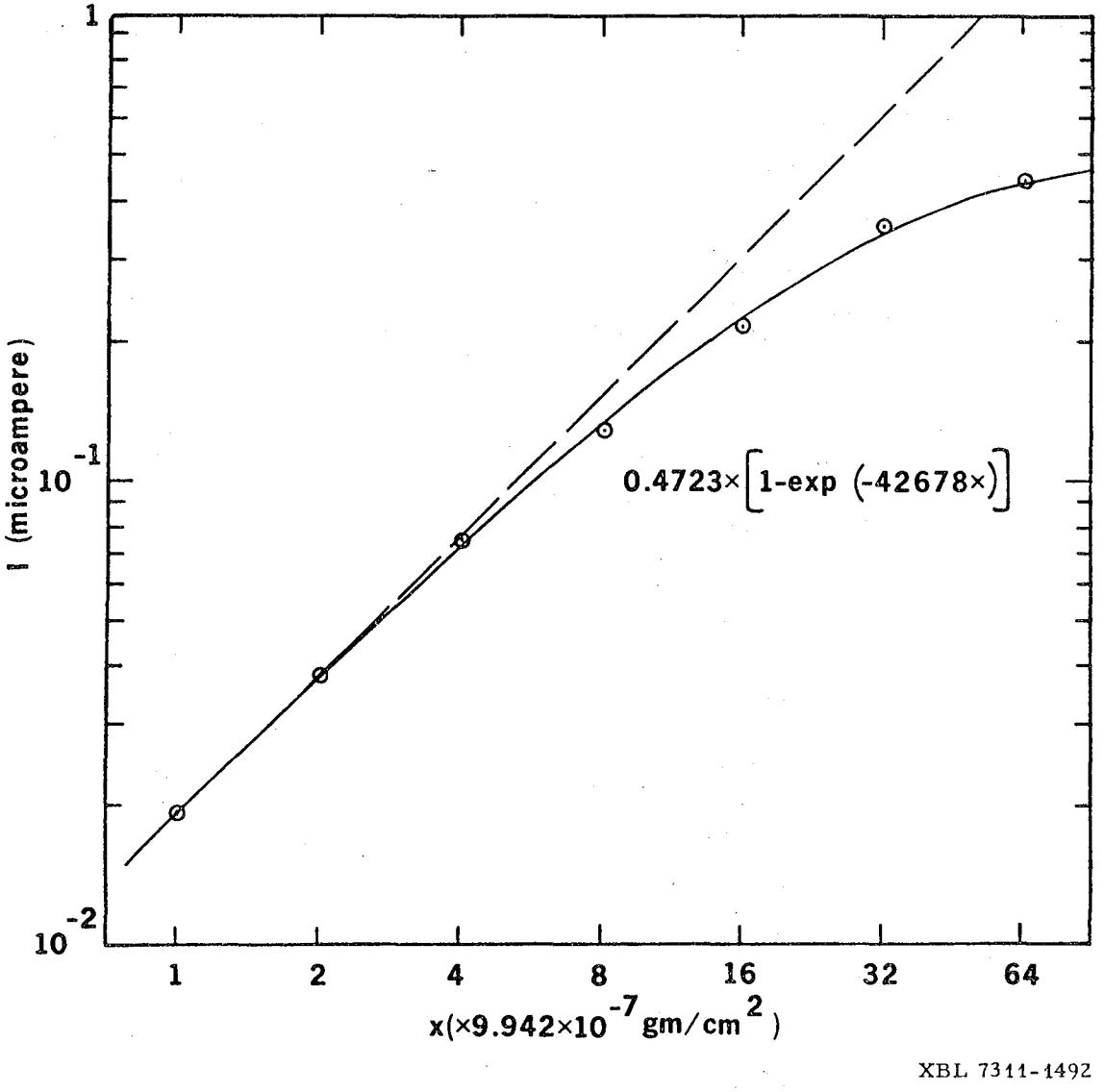


Fig. 4 Self-absorption effect in uranine solution

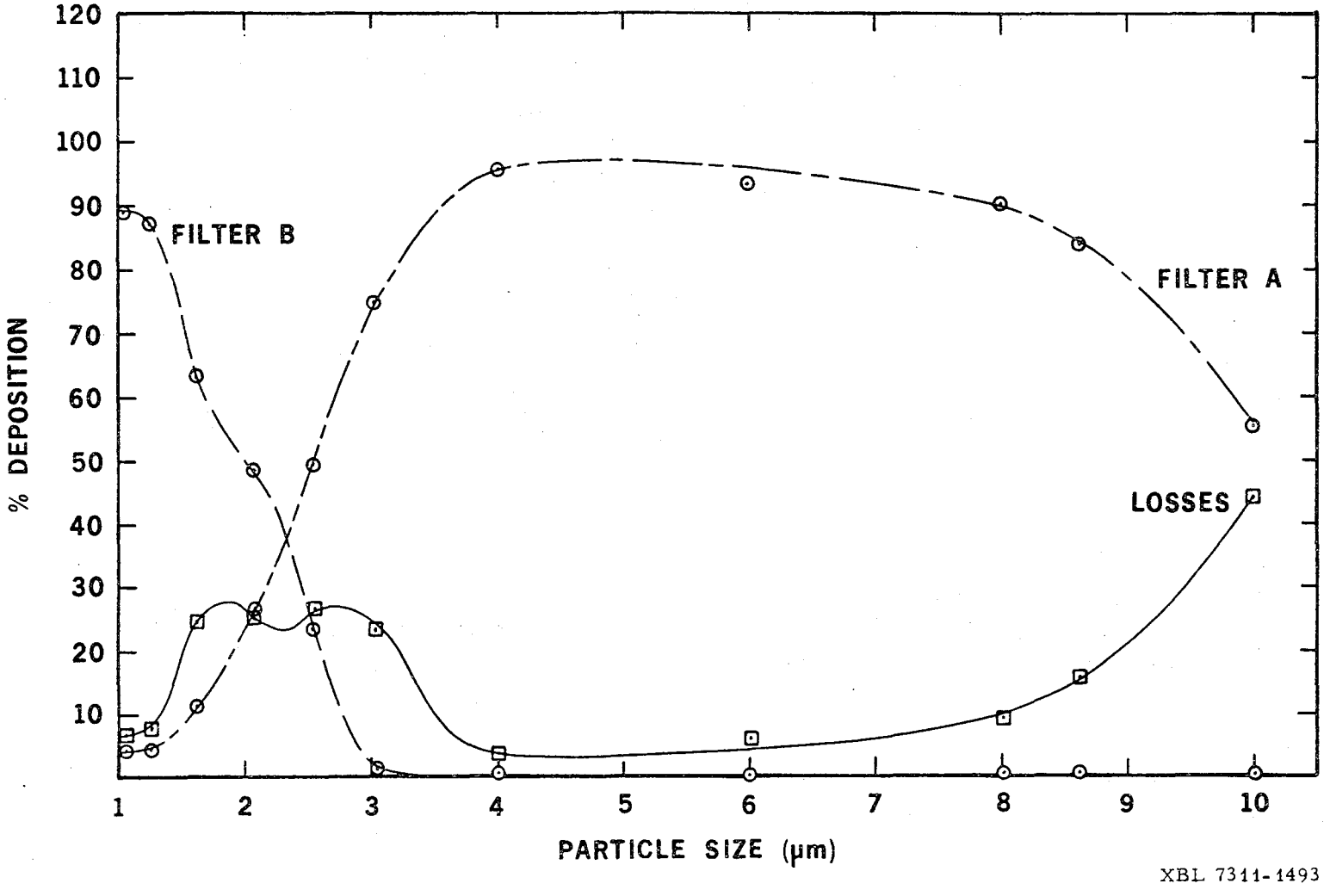


Fig. 5 Size separation characteristics and the total loss spectrum

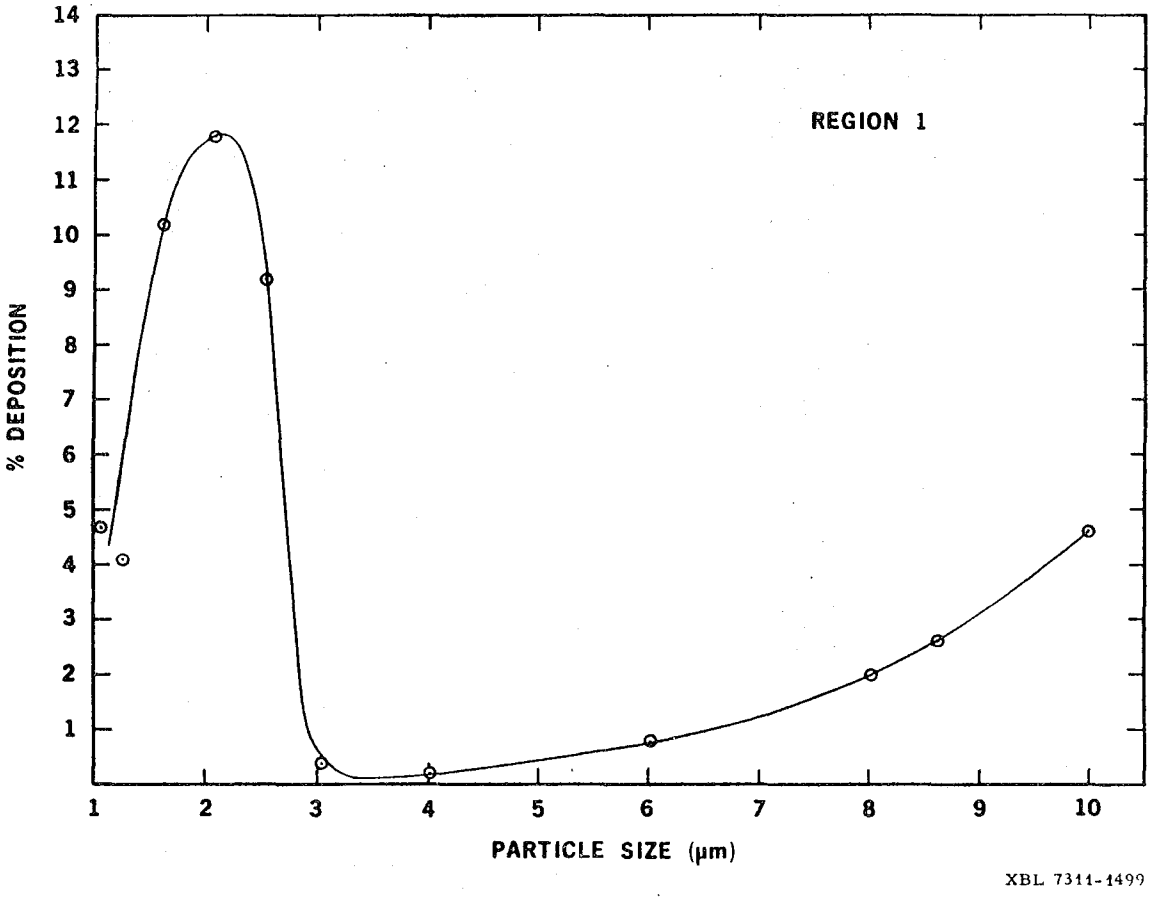


Fig. 6 Regional loss spectrum

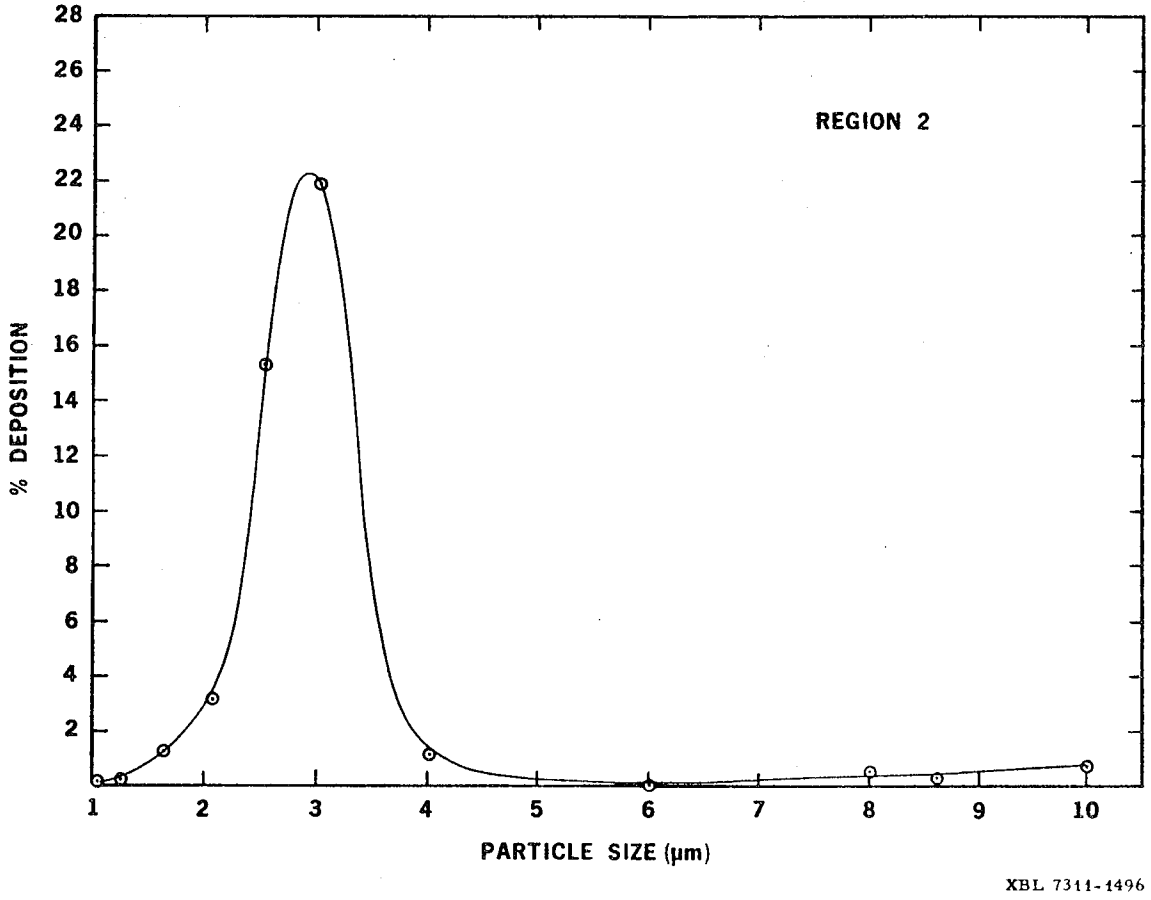


Fig. 7 Regional loss spectrum

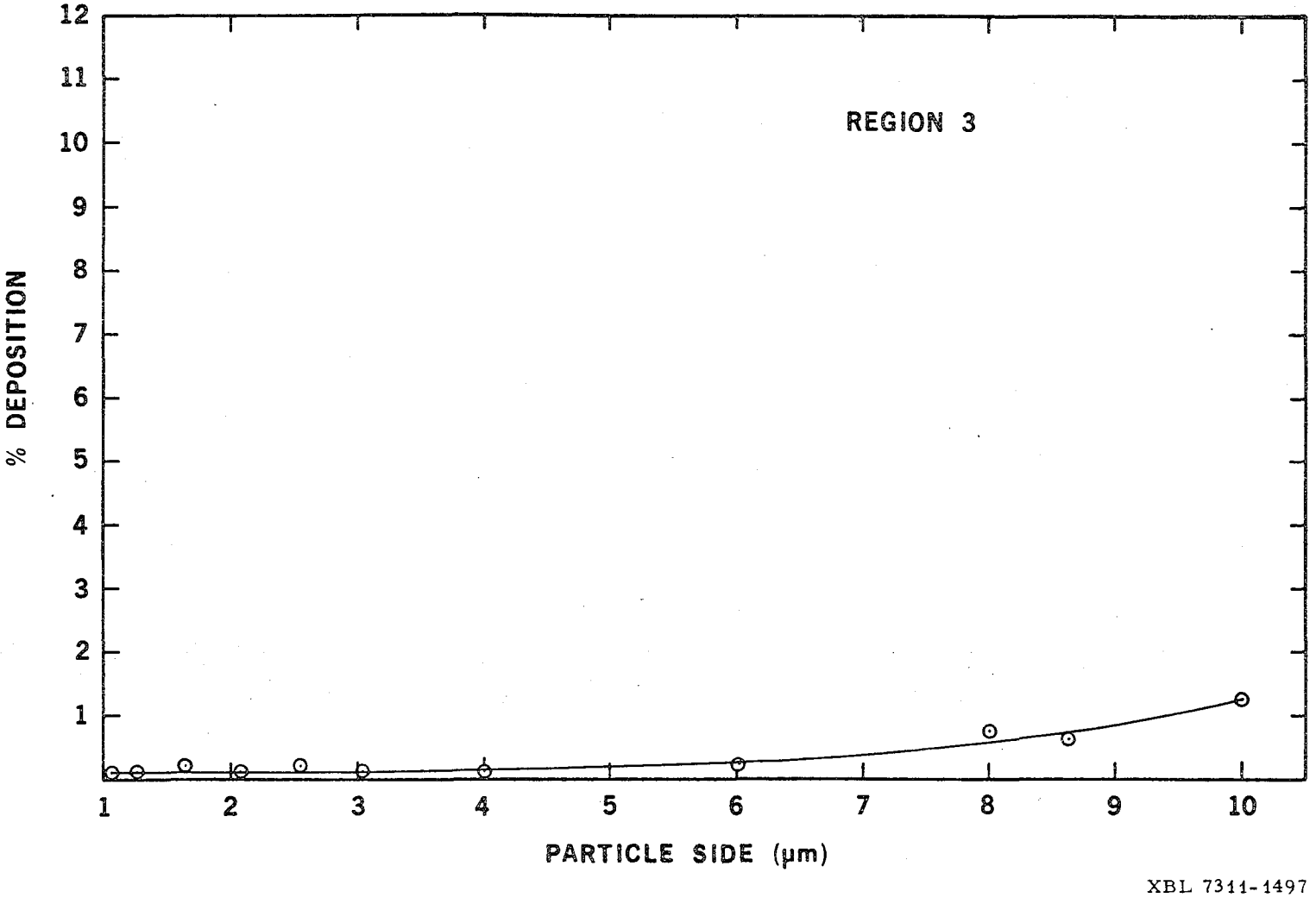
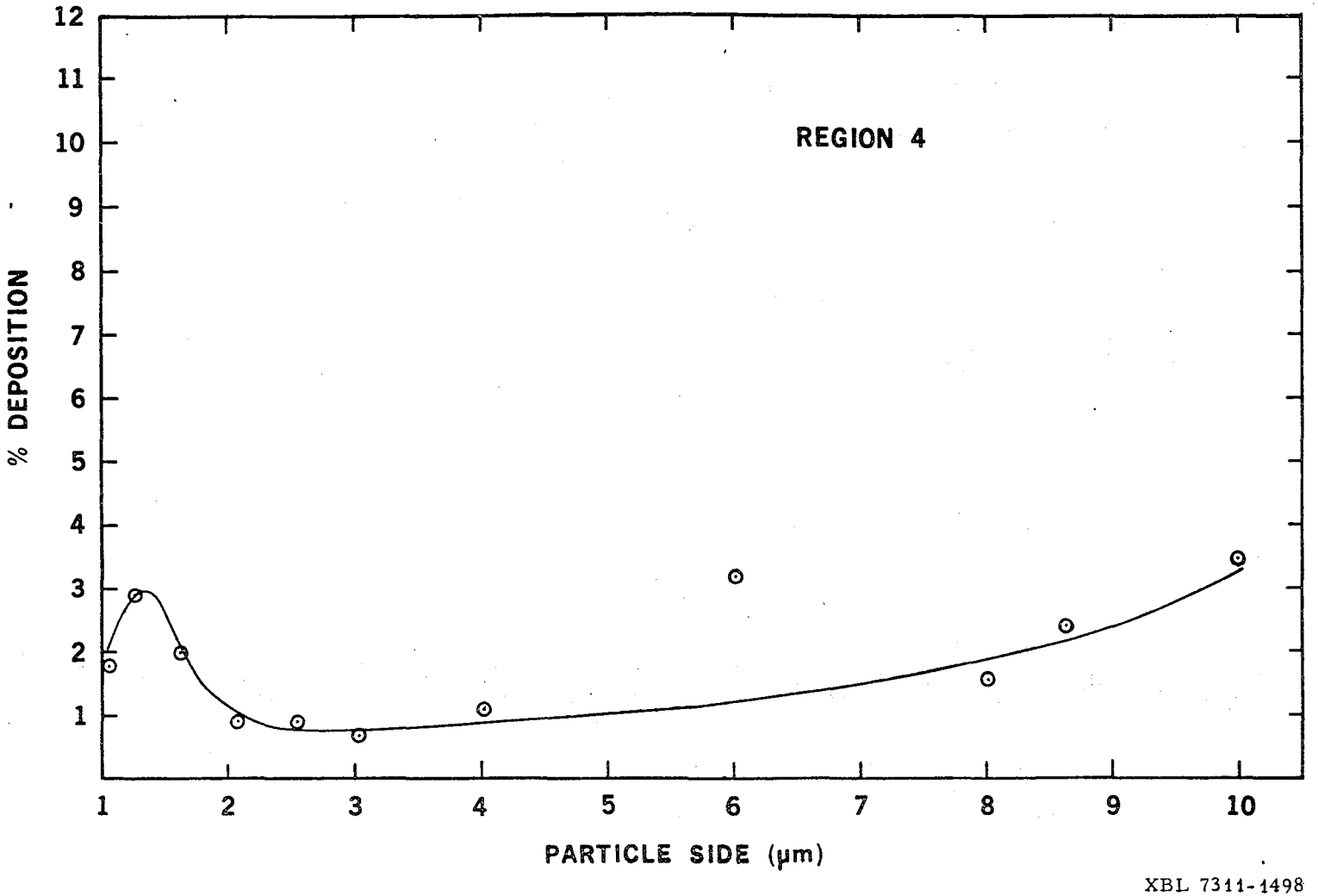


Fig. 8 Regional loss spectrum



XBL 7311-1498

Fig. 9 Regional loss spectrum

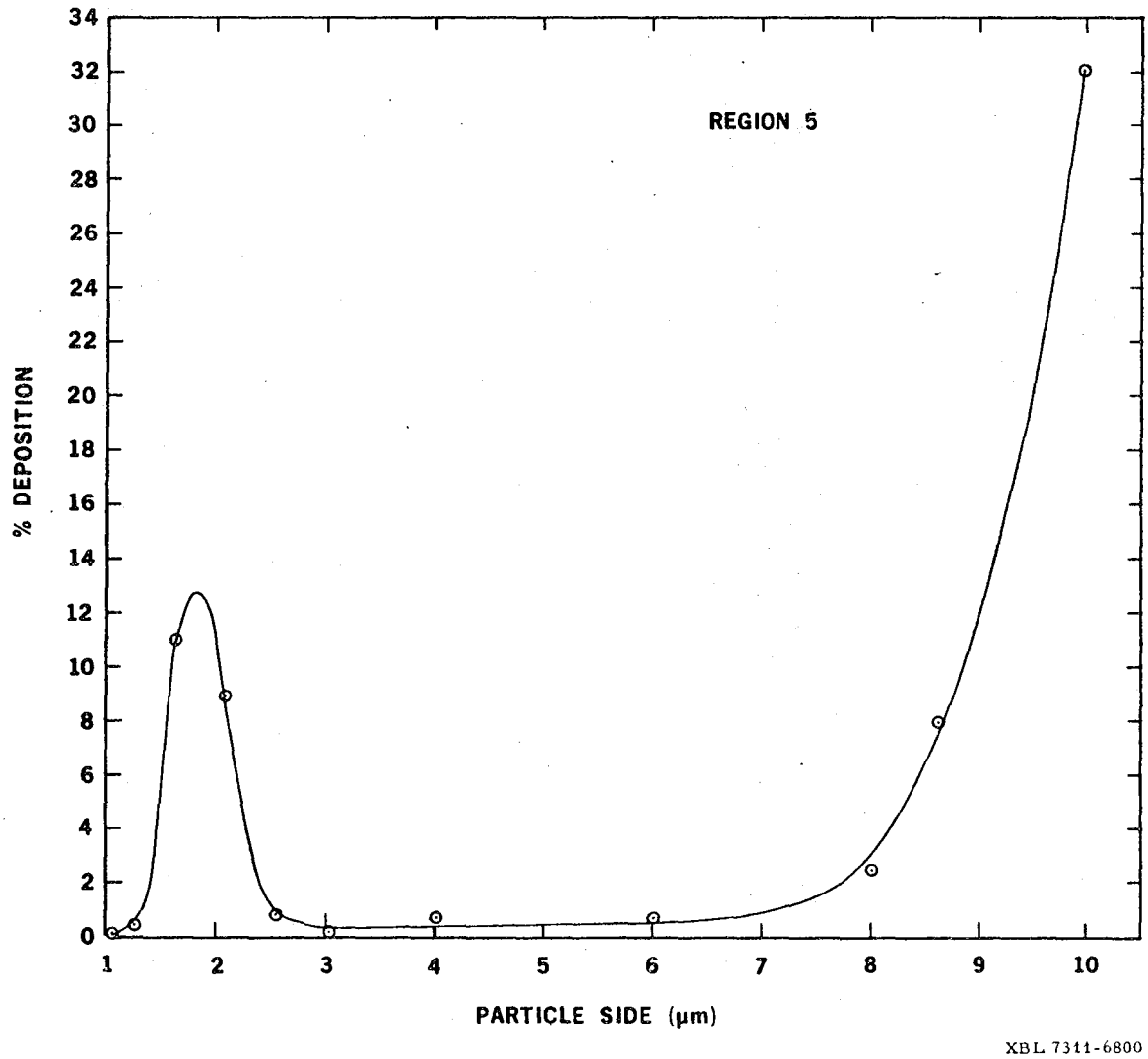


Fig. 10 Regional loss spectrum

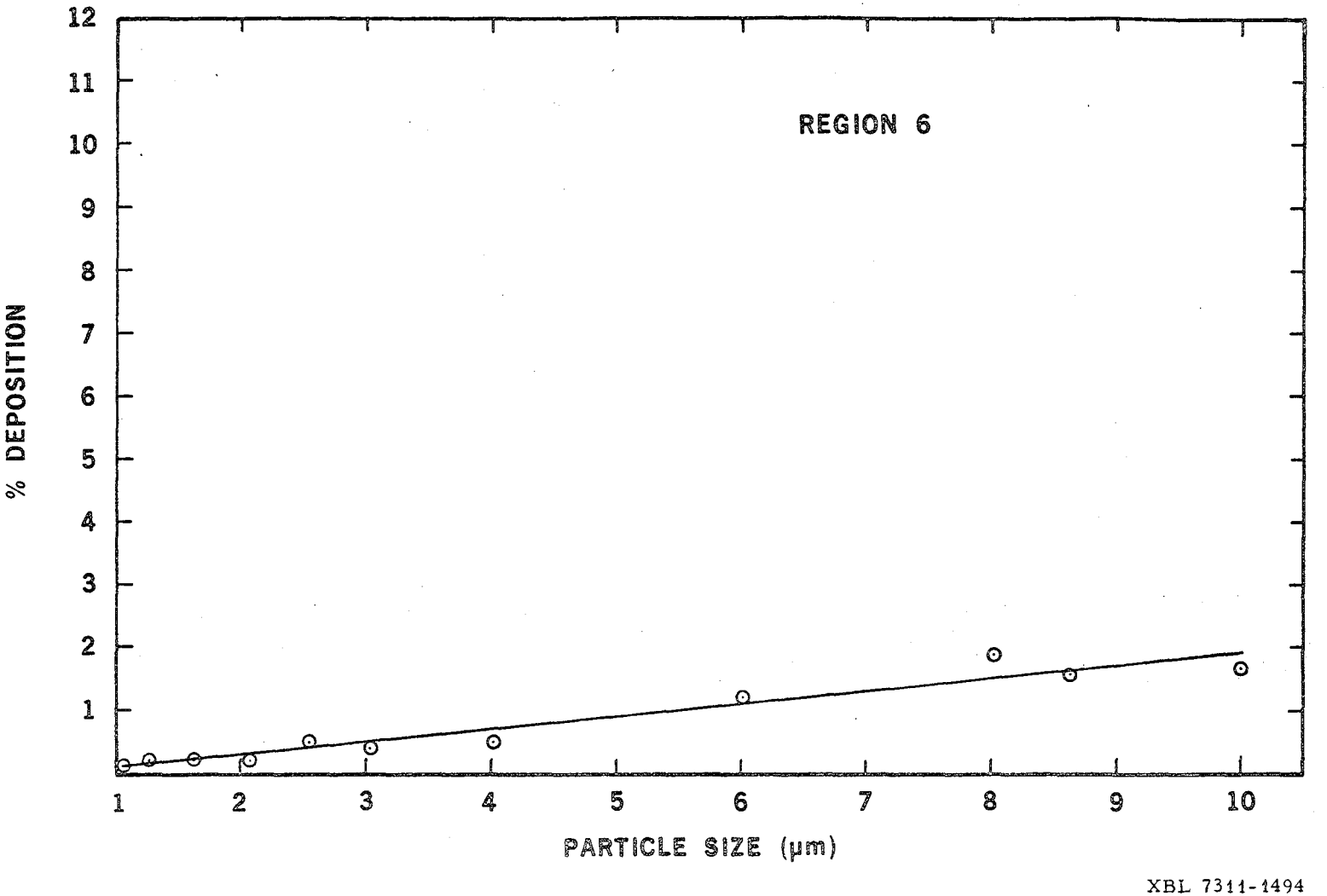


Fig. 11 Regional loss spectrum

LEGAL NOTICE

This report was prepared as an account of work sponsored by the United States Government. Neither the United States nor the United States Atomic Energy Commission, nor any of their employees, nor any of their contractors, subcontractors, or their employees, makes any warranty, express or implied, or assumes any legal liability or responsibility for the accuracy, completeness or usefulness of any information, apparatus, product or process disclosed, or represents that its use would not infringe privately owned rights.